



Aix-en-Provence, France, 24-26 September 2003

## EVALUATION ISSUES OF THERMAL MEASUREMENTS BASED ON THE STRUCTURE FUNCTIONS

M. Rencz<sup>1</sup>, E. Kollár<sup>2</sup>, A. Poppe<sup>1,2</sup>, S. Röss<sup>2</sup>

<sup>1</sup> MicReD Ltd., H-1112 Gulyás u.27, Budapest, Hungary  
<rencz|poppe>micred.com

<sup>2</sup> BUTE, Department of Electron Devices, H-1521 Goldmann Gy.tér 3, Budapest, Hungary  
<kollar|poppe|ross>@eet.bme.hu

### ABSTRACT

Measurement of different thermal properties is based on different features of the *structure functions* [1], [2] calculated from thermal transient curves measured at high accuracy. Structure functions are direct models of essentially one-dimensional heat-flow paths while in case of complex 3D heat-spreading they can be considered as equivalent models. In structure function based measurement evaluations the essentially one dimensional heat-flow is assured by special fixtures, however, there exist parasitic heat-flow paths resulting in losses parallel to the main flow. To assure 3..10% accuracy of the structure function based measurements one has to consider these losses and their effect should be subtracted from the structure functions obtained for the net system (main path + parasitic ones). This paper provides details of the applied computational method and provides a few practical examples.

### 1. INTRODUCTION

*Structure functions* [1], [2] are "graphical" representations of the RC-model of thermal systems. In case of essentially one-dimensional heat-flow (such as longitudinal flow in a rod or radial spreading in homogeneous material layers, or even in cylindrical or spherical spreading) structure functions can be considered as direct models of the thermal system. In practical cases the *cumulative structure function* is directly constructed from the Cauer-network equivalent RC model of the thermal system (Figure 1) as follows. The thermal resistance between the  $n$ -th element of the model network and the heat source (driving point) is

$$R_{\Sigma} = \sum_{i=1}^n R_i \quad (1)$$

and the cumulative thermal capacitance is

$$C_{\Sigma} = \sum_{i=1}^n C_i \quad (2)$$

where  $R_i$  and  $C_i$  denote the element values of the  $i$ -th stage of the Cauer-type model network. Plotting the  $C_{\Sigma n}$  vs.  $R_{\Sigma}$  values results in the *cumulative structure function* (Figure 2). It can be proved, that the derivative of  $C_{\Sigma}(R_{\Sigma})$ , the *differential structure function*

$$k = \frac{dC_{\Sigma}}{dR_{\Sigma}} \quad (3)$$

is proportional to the square of the cross-sectional area of the conducting path. We obtain such Cauer-ladders from Foster-models that are directly calculated from the discretised time-constant spectrum of the thermal system.

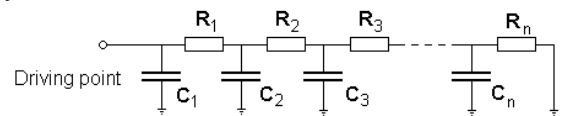


Figure 1: Cauer-type network model of a thermal impedance.

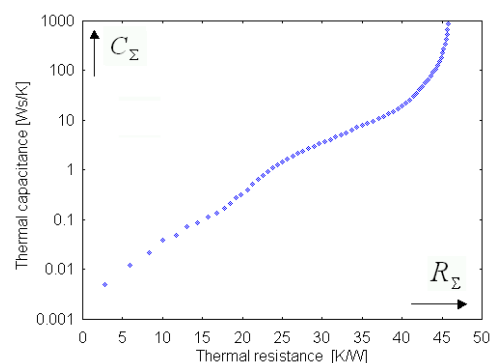


Figure 2: Cumulative structure function of a heat-flow path. The left-hand side corresponds to the driving point, the right-hand side to the ambience.

Structure functions are well applicable to identify *characteristics of certain elements of the heat-flow path*, since for different types of essentially one-dimensional heat-flow the corresponding structure functions show specific features. E.g. radial heat-flow in a disk appears in the corresponding cumulative structure function as a straight line with a given slope where the slope is proportional to the thickness and to the thermal conductivity of the disk [3]. Thus, with a fixture assuring radial heat-flow in PCB-s allows the indirect measurement of the average (effective) thermal conductivity of the board [3].

Placing samples into special fixtures and making highly accurate thermal transient measurements, the corresponding structure functions provide means for the indirect measurement of their thermal properties. Such indirect measurements are accurate if the heat-flow from the driving point to the ambient is a purely one-dimensional flow. Unfortunately, there are always "parasitic" parallel heat-flow paths present even in structures designed to be dominantly one-dimensional, see Figure 3. Such parasitic losses are realised e.g. by natural convection, or the fixture itself.

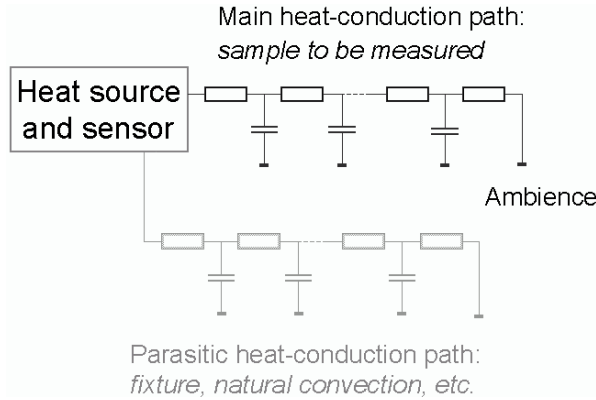


Figure 3: Main heat-flow path and a parallel parasitic heat-flow path

In order to re-gain the accuracy of the structure-function based indirect measurements, the effect of these parallel paths has to be accounted for while creating or using the structure functions for measurement.

## 2. CONSIDERING THE EFFECT OF A PARALLEL HEAT-FLOW PATH

Figure 4 shows measuring a  $Z(s)$  thermal impedance. This  $Z(s)$  impedance is constituted by the "ideal"  $Z^*(s)$  thermal impedance *to be identified* and the thermal impedance of the shunting heat-flow path. For the sake of simplicity we restrict our discussion now to a purely resistive branch with an  $R$  thermal resistance.

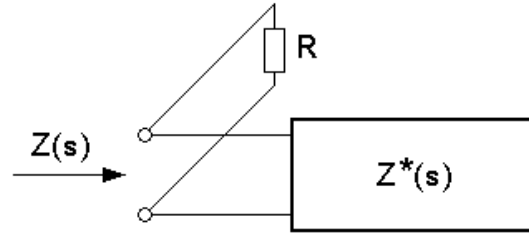


Figure 4: "Ideal"  $Z^*(s)$  thermal impedance to be identified together with a shunting thermal resistance  $R$

The measured thermal impedance – described by a Foster-model derived directly from the time-constant spectrum – can be written as follows:

$$Z(s) = \sum_{i=1}^N \frac{R_i}{1 + s t_i} \quad (4)$$

where  $R_i$  and  $t_i$  are the resistance and time-constant values of the Foster-stages, respectively. Rewriting it into a quotient of two polynomials yields

$$Z(s) = \frac{n_0 + n_1 s + n_2 s^2 + \dots}{d_0 + d_1 s + d_2 s^2 + \dots} = \frac{\sum_{i=0}^{N-1} n_i s^i}{\sum_{i=0}^N d_i s^i} \quad (5)$$

where  $n_i$  and  $d_i$  are the coefficients of the numerator and denominator polynomials, respectively. In case of parallel impedances the effect of  $R$  can be easily accounted for if the impedances are replaced by their reciprocals:

$$\begin{aligned} \frac{1}{Z^*(s)} &= \frac{1}{Z(s)} - \frac{1}{R} = \frac{\sum_{i=0}^N d_i s^i}{\sum_{i=0}^{N-1} n_i s^i} - \frac{G \sum_{i=0}^{N-1} n_i s^i}{\sum_{i=0}^{N-1} n_i s^i} = \\ &= \frac{\sum_{i=0}^{N-1} (d_i - G n_i) s^i + d_N s^N}{\sum_{i=0}^{N-1} n_i s^i} \end{aligned} \quad (6)$$

where  $G = 1/R$ . The correction accounting for the effect of  $R$  is to be carried out in the phase of generating the structure functions, when the thermal impedance is available in the form as given by formula (4) – that is during the Foster-Cauer transformation of the RC model of the impedance [1]. The following transformations need to be done in the coefficients of the numerator and denominator polynomials:

$$\begin{aligned} d_i^* &= d_i - G \cdot n_i \quad \text{if } i = 0 \dots N-1 \\ d_N^* &= d_N \end{aligned} \quad (7)$$

The calculations are similar when the shunting "branch" is not purely resistive but it is characterised by a thermal impedance with various time-constants, given in the form corresponding to (4).

### 3. MEASUREMENTS BASED ON STRUCTURE FUNCTIONS: EXAMPLES

#### 3.1. Measuring the effective thermal conductivity of PCB-s

This measurement is based on the evaluation of the *cumulative structure function*. A special fixture is attached to the *T3Ster* thermal transient test equipment [4]: the board to be measured is inserted below a transistor ending in a tip and an isothermal ring surrounding this tip (see Figure 5). The transistor acts as a heater and as a sensor. This arrangement assures radial heat-flow in the board between the tip and the isothermal ring. From the thermal transient of the heating/sensing transistor captured by the *T3Ster* equipment the cumulative structure function is derived. The section of the structure function that corresponds to the radial spreading in the PCB is a straight line segment next to the singularity, at the end of the function [3]. Figure 6 shows a structure function with the effective thermal conductivity measured this way.

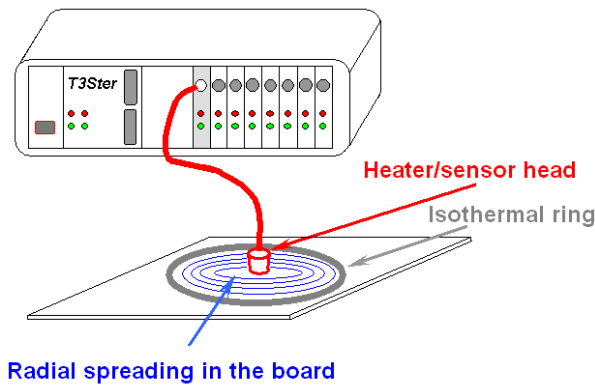


Figure 5: Schematic of the setup for measuring board thermal conductivity

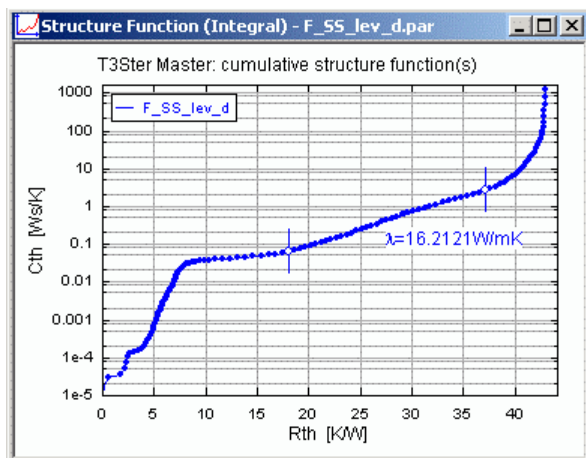


Figure 6: Measurement of the effective board thermal conductivity in the cumulative structure function

In this measurement natural convection taking place at the board surface causes a parallel heat-flow path on one hand, on the other hand the measuring fixture itself, via the powering structure as shown in Figure 7.

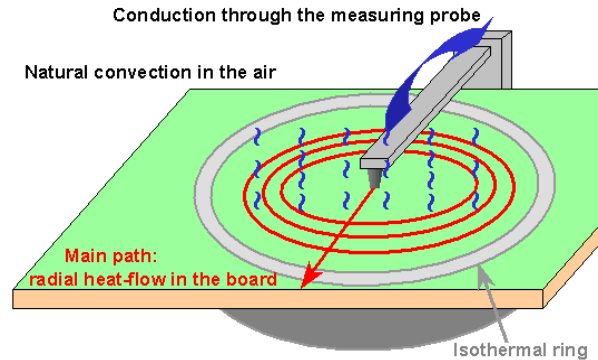


Figure 7: Parasitic parallel heat-flow paths in the effective board thermal conductivity measurement setup

The effect of all these can be lumped into a single shunting conductance. Both effects can be exactly identified if a calibration board is placed into the fixture and is measured in vacuum and in a still air chamber: the shunting conductance in the latter case is the correction value to be considered in all subsequent measurements of other boards. This shunting conductance represents both the conduction through the fixture and the heat-loss through natural convection. Figure 8 presents cumulative structure functions for a measurement of a PCB with and without this correction.

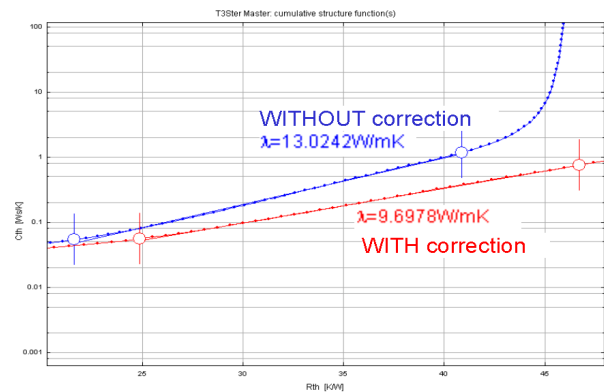
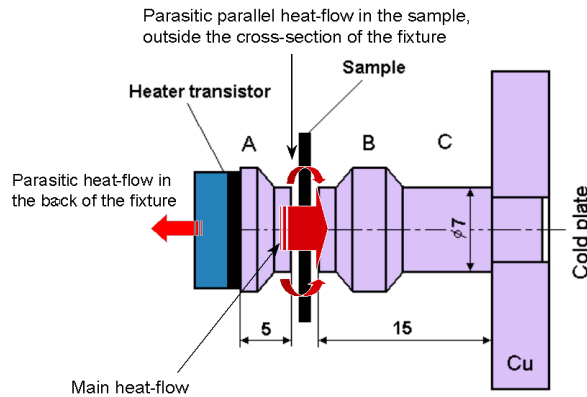


Figure 8: Measured effective board thermal conductivity without and with parasitic heat path correction

#### 3.2. Measurement of thermal resistance of interface materials

This measurement [5] is based on the use of the *differential structure functions* [1]. First the reference function of the empty fixture is identified, then the one with the sample. The measurement principle is based

on the shift of peaks in the differential structure function of the fixture as illustrated by Figure 9 and Figure 10.



*Figure 9: Fixture for measuring thermal resistance of interface materials, indicating possible parasitic heat-flow paths.*

The peak corresponding to section B shifts with respect to the peak belonging to section A as a sample is inserted into the fixture. The physical arrangement, together with the main and parasitic parallel heat-flow paths is also shown in Figure 9.

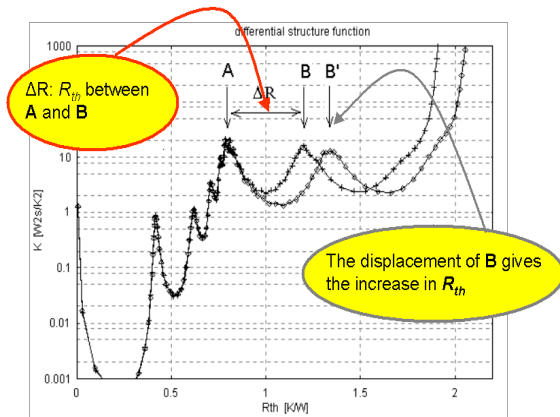


*Figure 10: Displacement of peak B in the differential structure function gives the thermal resistance of the sample*

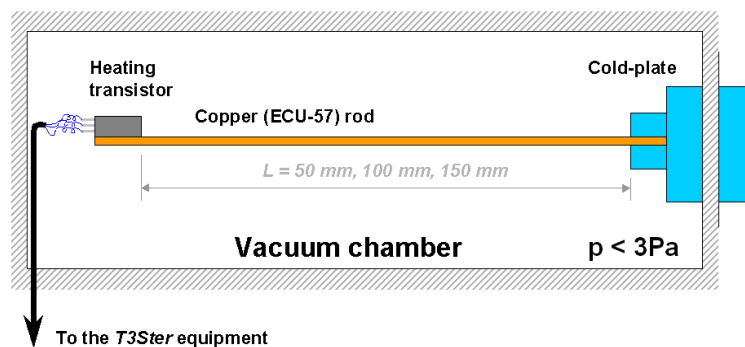


*Figure 11: Setup for the measurement of the thermal conductivity of a copper (ECU-57 or C11000) rod*

According to our simulation studies the parasitic heat-flow within the sample material outside the cross-section of the fixture is negligible. The heat-flow in a shunting path at the back of the fixture again can be identified in a calibrating measurement and later on, as a single resistive loss, as described in section 2.

#### 4. A SIMPLE CASE STUDY

We demonstrate the effects of parasitic heat-flow paths on our measurements in a simple case study. We measured a copper rod both in vacuum and in still air chamber as shown Figure 11. The rod with a rectangular cross section was made of a standard material denoted as ECU-57 (C11000 in the USA or C1100 in Japan), for which the text-book value of the  $\lambda$  thermal conductivity is given between 385W/Km [6] and 391W/Km [7]. We have considered the value of 388W/Km @ 20°C, also used in [8]. The width of the rod was  $a=12\text{mm}$ , and its thickness was  $b=0.99\text{mm}$ . A power transistor (BD245) was attached to one end of the rod while the other end was fixed to a cold-plate. The arrangement assured a perfect one-dimensional (longitudinal) heat-flow inside the rod. The whole structure was placed into a vacuum chamber in order to eliminate convection losses. The vacuum chamber exposed to atmospheric pressure served as a still air chamber. In order to minimise the parasitic heat-flow across the electrical connections of the bipolar transistor thin connection wires were applied. With the T3Ster equipment we measured different thermal transients as follows:

- "empty" transistor in vacuum ( $p < 3\text{Pa}$ ),
- transistor with the rod attached with three different transistor to cold-plate lengths ( $L=50\text{mm}$ ,  $100\text{mm}$  and  $150\text{mm}$ ) in vacuum ( $p < 3\text{Pa}$ ),
- the same transistor to cold-plate lengths as above, at atmospheric pressure (corresponding to a still-air chamber).

In Figure 12 we present the differential structure functions for the rod obtained in a still air chamber and in a vacuum chamber. In the differential structure function it is easy to locate the valley corresponding to the interface thermal resistance between the transistor package body and the rod. In the function plots we "measure" the thermal resistance of the rod from this interface (second vertical line from the left in the plot).

a [m]	0.01200		
b [m]	0.00099		
$\lambda$ [W/Km]	388	A [m <sup>2</sup> ]	0.00001188
L <sub>1</sub> [m]	0.05000	R <sub>th1</sub> [K/W]	10.85
L <sub>2</sub> [m]	0.10000	R <sub>th2</sub> [K/W]	21.69
L <sub>3</sub> [m]	0.15000	R <sub>th3</sub> [K/W]	32.54

*Table 1: Main parameters of the copper (ECU-57 or C11000) rod – thermal resistance values are calculated from geometry and from the known  $\lambda$  thermal conductivity value [8].*

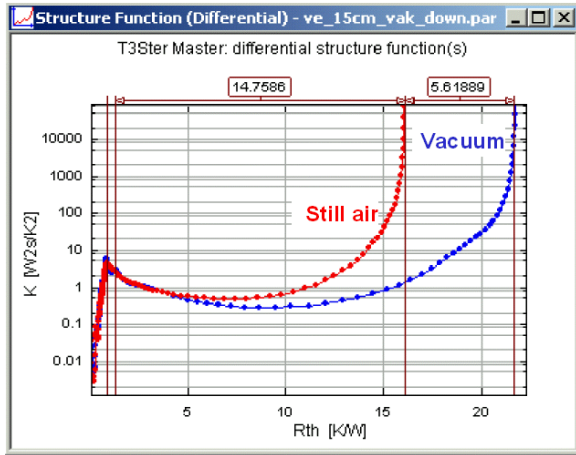


*Figure 12: Differential structure functions calculated from still air and vacuum chamber measurement results for the 150mm long copper (ECU-57) rod, measured according to the setup shown in Figure 11.*

For the still air case we obtain a smaller total value for the thermal resistance ( $R_{thair}=14.76$  K/W), since cooling via natural convection realises an extra heat-flow path. For the vacuum case a higher thermal resistance value can be read ( $R_{thvac}=14.76+5.62=20.37$  K/W). The  $R_{conv}$  thermal resistance corresponding to the natural convection can be written as

$$\frac{1}{R_{thvac}} + \frac{1}{R_{conv}} = \frac{1}{R_{thair}} \quad (8)$$

thus, for  $R_{conv}$  we obtain a value of 53.59 K/W. The total area of the rod exposed to air is  $A_{total} = 2L(a+b) = 0.003897\text{m}^2$ . With these values a heat transfer coefficient value  $HTC=1/(R_{conv} \cdot A_{total}) = 4.788\text{W/Km}^2$  can be calculated – a value very close to  $5\text{W/Km}^2$  usually considered as an HTC in still air.

In the second series of measurements we tried to identify the  $\lambda$  thermal conductivity of the rod from measured transients. All measurements (with  $L_1=50\text{mm}$ ,  $L_2=100\text{mm}$  and  $L_3=150\text{mm}$ ) were carried out in vacuum. In each case heat-conduction from the junction to the ambience took place through the rod (main path) and through the electrical connections of the transistor (parasitic path). The thermal resistance values read from the structure functions of Figure 13 are considerably less than the theoretical values given in Table 1. This is due to the shunting heat-conduction path realised by the electrical connections of the transistor. The thermal resistance of that parasitic path has also been identified: it can be read from the structure function that was derived from the thermal transient of the free-standing "empty" transistor measured in vacuum (Figure 14). With that value (cca.  $66.34\text{K/W}$ ) we applied the correction method discussed in section 2.

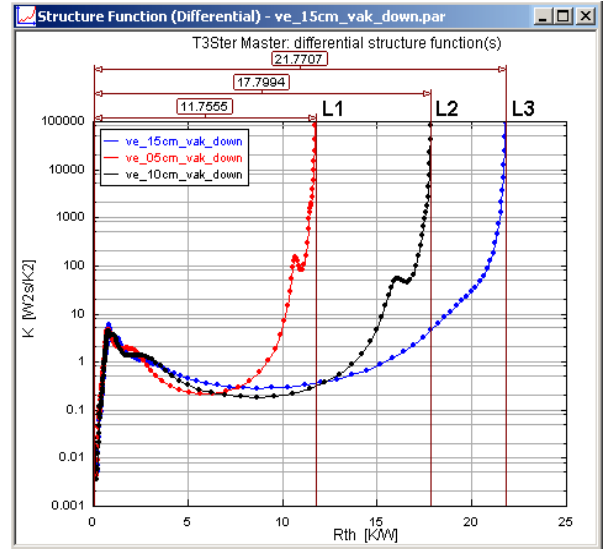


*Figure 13: Differential structure functions for the total chip-to-ambient heat-flow through the copper rod at lengths of  $L_1$ ,  $L_2$  and  $L_3$ .*

The structure functions corresponding to the  $L_3=150\text{mm}$  case are shown in Figure 15. The thermal resistance corresponding to the 150mm long copper rod is the distance between the peak on the right hand side of the case-to-rod thermal interface and the singularity of the plot (corresponding to the ambience):  $31.16\text{K/W}$ . This is close to the  $R_{th3} = 32.54\text{K/W}$  thermal resistance value given in Table 1. The relative error of the thermal resistance identified this way is 4.25%. Calculating back the  $\lambda$  thermal conductivity of the ECU-57 material from the measured thermal resistance results in a value of  $\lambda_{meas} = 405.2$  W/Km which is also very close to the text-book value of  $388\text{W/Km}$  (with a similar relative error as above).

After carrying out the same sort of correction for the thermal resistances obtained for the  $L_1$  and  $L_2$  lengths of the rod we obtain  $R_{th2}/R_{th1}$  and  $R_{th3}/R_{th1}$  ratios very close to 2 and 3, respectively – as expected from the geometrical ratios (see Table 1).

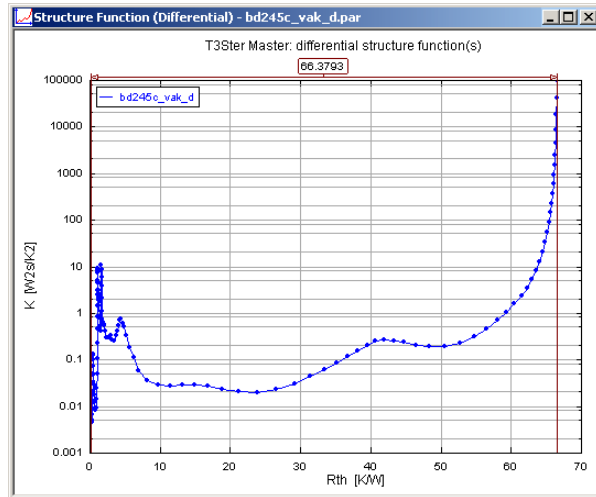


Figure 14: Differential structure function of the "empty" transistor standing free in vacuum.

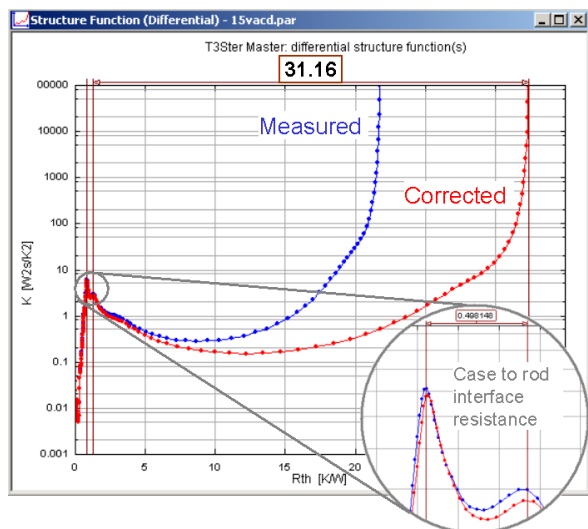


Figure 15: Differential structure functions corresponding to the 150mm long copper (ECU-57) rod, measured in vacuum.

## 5. CONCLUSIONS

In this paper we demonstrated, that it is possible to subtract the thermal impedance (admittance) of shunting branches from structure functions.

This option is very important when in case of structure function based indirect measurement of materials thermal properties we want to diminish the effect of parasitic heat-flow paths. Such parasitic paths always do exist even in case of special fixtures accu-

rately designed to assure one-dimensional heat-flow. Parasitic effects are e.g. natural convection which and conduction through the fixture itself which considerably influence the results of measurement of e.g. the effective board thermal conductivity.

With a simple set of experiments in a vacuum chamber we have demonstrated the effect of natural convection as well as parasitic heat-flow via the electrical connections of a heating and measuring transistor. The presented examples also demonstrated the applicability of our correction method. With these simple experiments we also demonstrated the applicability of the structure function based measurement methods, since the identified HTC and  $\lambda$  values were very close to the widely known text-book values.

## 6. ACKNOWLEDGEMENTS

This work was supported by the NKFP 2/018/2001 "INFOTERM" project of the *Hungarian Government*. We are grateful to János Mizsei who provided access to a vacuum chamber for our measurements. Thanks are also due to *ABM Hungária Kuprál Ltd*, the local branch of *Austria Buntmetall* for providing us the copper material samples.

## 7. REFERENCES

- [1] V. Székely and Tran Van Bien: "Fine structure of heat flow path in semiconductor devices: a measurement and identification method", *Solid-State Electronics*, V.31, pp.1363-1368 (1988)
- [2] [www.micred.com/strfunc.html](http://www.micred.com/strfunc.html)
- [3] V. Székely, M. Rencz, S. Török, S. Ress: "Calculating effective board thermal parameters from transient measurements" *IEEE Tr. on Components and Packaging Technologies*, Vol 24, No 4, Dec.2001, pp 605-610.
- [4] [www.micred.com/t3ster.html](http://www.micred.com/t3ster.html)
- [5] M. Rencz, V. Székely: "Measuring partial thermal resistances in a heat flow path", *IEEE Tr. on Components and Packaging Technology*, Vol 25, No 4, Dec. 2002, pp 547-553
- [6] [www.ozar-metal.com/html%5Cfiyat.html](http://www.ozar-metal.com/html%5Cfiyat.html)
- [7] [www.casti.ca/books\\_ebooks/lite/RedBookLite.pdf](http://www.casti.ca/books_ebooks/lite/RedBookLite.pdf)
- [8] S. G. Kandlikar, M. E. Steinke, A. Singh: "Effects of Weber number and surface temperature on the boiling and spreading characteristics of impinging water droplets", In Proceedings of NHTC'01 – the 35<sup>th</sup> National Heat Transfer Conference, June 10-12 2001, Anaheim, California, USA, paper # NHTC01-11672, also at [www.rit.edu/~taleme/69-NHTC01-11672.pdf](http://www.rit.edu/~taleme/69-NHTC01-11672.pdf)